Iranian Journal of Chemical Engineering
Vol. 9, No. 3 (Summer), 2012, IAChE

Methane Combustion and CO Oxidation on Ag-Doped $LaMn_{0.8}Cu_{0.2}O_{3\pm\delta}$ Mixed Oxides Prepared by Pechini and Sol–Gel Methods

M. Abdolrahmani, M. Parvari, M. Habibpoor*
School of Chemical Engineering, Iran University of Science and Technology, Tehran, Iran.

Abstract

Lanthanum in the A-site of $LaMn_{0.8}Cu_{0.2}O_{3\pm\delta}$ perovskite was partially substituted by silver. $La_{1-x}Ag_xMn_{0.8}Cu_{0.2}O_3$ samples (x=0, 0.1, 0.2, 0.3) were prepared by the two Pechini and sol–gel methods and their catalytic activity was evaluated for CH_4 combustion and CO oxidation reactions. FT-IR analysis of different samples before calcination confirmed the formation of different complexes between the elements. Calcined samples were characterized using XRD, TPR, BET, SEM and XRF techniques. XRD results revealed that the Pechini method led to perovskite structures with higher purity and that segregation of Ag in samples prepared by the sol–gel method was higher. SEM images and EDS results for samples before and after catalytic tests showed that the Pechini samples had a lower particle size and better distribution of the elements. The catalytic results indicate that the oxidation activity increased with the amount of Ag in the oxide, but the stability of the structure decreased.

Keywords: *Perovskite, Pechini Method, Sol–Gel Method, Oxidation Catalyst*

1. Introduction

The catalytic combustion process has been developed over a variety of catalytic systems to pursue suitable catalysts with high thermal stability and activity [1]. Perovskite-type oxides of the general formula ABO_3 are well-known catalysts for the catalytic combustion of methane and catalytic oxidation of CO [2]. Tailoring of their catalytic properties and thermal stability by partial substitution of A and/or B sites [3, 4, 5] can yield perovskites that are over-stoichiometric or deficient in oxygen under well-defined conditions [6]. Many metallic elements are stable in the perovskite structure provided that the A and B ions have dimensions (r_A>0.90 Å, r_B>0.51 Å) consistent with the limits of the so-called tolerance factor t ($0.8<t<1.0$) defined by Goldschmidt as $t= (r_A+r_O)/\sqrt{2}\ (r_B+r_O)$, where r_A, r_B, and r_O are the ionic radii for A, B, and O, respectively [7]. The distance between the cation and oxygen is related only to the oxidation state of the cation and to the nature of occupied sites [8]. If t is somewhat different, the cubic structure will be distorted and an orthorhombic or rhombohedral

* Corresponding author: Parvari@iust.ac.ir

structure is obtained [9]. Up to now, almost all known perovskite compounds have *t* values in the range of 0.75–1.00. However, it seems that *t* = 0.75–1.00 is not a sufficient condition for the formation of the perovskite structure, as indicated later, for some systems whose *t* are even within the most favorable range (0.8–0.9), no perovskite structure is stable[10].

It has been reported that perovskites of the structural formula $LaBO_3$ with B=Mn, Co or Ni are particularly suitable for total VOC oxidation [11, 12, 13]. The lanthanide ions at A sites are generally catalytically inactive, whereas the activity of unsubstituted ABO_3 is mainly determined by component B of transition metals [3]. Partial substitution of ions in positions A and/or B for A' and B' produces crystal lattice defects or creates O^{2-} vacancies in the lattice, thus enhancing the catalytic properties of such catalysts [2]. Studies on the effect of lanthanum substitution by divalent elements such as Sr, Ce and Ca [14, 15, 16, 17] and monovalent elements such as Na and K [18, 19, 20, 21] have been widely reported during the last decade. Also, the substitution of La in $LaMnO_3$ by Ba, Pb was reported to enhance the catalytic activity in full oxidation reaction of CO and hydrocarbons [22].

Perovskite-type manganese oxides are widely used as catalysts in environmental reactions such as the conversion of carbon monoxide and hydrocarbons [5]. High activity for the combustion of hydrocarbons is characteristic of catalysts in which the metal in position A has been substituted with silver, such as $La_{0.7}Ag_{0.3}Fe_{0.5}Co_{0.5}O_3$, $La_{0.7}Ag_{0.3}FeO_3$ [14] and $La_{0.7}Ag_{0.3}MnO_3$, which exhibited higher activity for methane combustion than $La_{0.7}Sr_{0.3}MnO_3$ [16]. Partial substitution of lanthanum with palladium or silver in $LaCoO_3$ perovskite enhanced the activity for methane combustion [23]. E. Gulari et al [24] demonstrated that composite silver cobalt oxide is a good CO oxidation catalyst. Song et al. [16] reported that $La_{0.7}Ag_{0.3}MnO_3$ would be a good candidate for cleaning and combustion of exhaust gases at low temperature.

Since the catalytic properties of materials are strongly dependent on the preparation procedure, it is essential to investigate the structure of perovskites prepared by the different methods. Perovskites can be synthesized by several methods. The methods, including thermal treatment at T >1000°C, are not suitable for catalytic applications since the high temperature leads to a material with low surface area [25]. Low-temperature synthesis routes such as co-precipitation [26] and flash combustion [27, 28] yield a relatively high surface area. Therefore, other methods for preparing perovskite-type oxides with higher BET surface area need to be identified [29].

$LaMn_{1-x}Cu_xO_3$ perovskites have been considered as catalysts for methane combustion and CO oxidation [30, 31, 32, 33]. Our previous work was focused on Mn substitution by copper in $LaMnO_3$ structure, and optimizing the Cu content in it. The results showed that partial substitution of copper had a positive effect on promoting reduction behavior of Mn which is, consequently, the reason for its promoted activity. It was observed that the optimized Cu to Mn ratio is 1 to 4 [38]. Therefore, from our previous study, $LaMn_{0.8}Cu_{0.2}O_{3\pm\delta}$ is chosen for further optimization and

comparison. In the present study, the effects of La substitution by Ag in $LaMn_{0.8}Cu_{0.2}O_{3\pm\delta}$ and its preparation method on catalyst morphology and activity in methane combustion and CO oxidation is investigated. Samples were prepared by the Pechini and sol–gel methods. The Pechini method involves the formation of a rigid polymer network between citric acid and ethylene glycol, which leads to a material with high degree of molecular homogeneity, as well as finer powders, thus presenting a higher surface area; essential property for catalyst reaction according to Fourier-transform infrared (FT-IR) spectroscopy, X-ray diffraction (XRD), X-ray fluorescence (XRF), scanning electron microscopy (SEM), energy-dispersive spectroscopy (EDS) and Bruner Emmet Teller (BET) analyses. For the purpose of comparison a sol-gel route using a chelating agent (like citric acid) is considered a useful technique because it presents the advantages of allowing low temperature and short periods of calcinations.

2. Experimental procedure

2-1. Preparation

Two methods, shown in Fig. 1(A, B), have been used to investigate the effect of preparation method on properties of $La_{1-x}Ag_xMn_{0.8}Cu_{0.2}O_{3\pm\delta}$ (x=0, 0.1, 0.2, 0.3) mixed oxides. $La_{1-x}Ag_xMn_{0.8}Cu_{0.2}O_{3\pm\delta}$ perovskite oxides were prepared using $La(NO_3)_3{\cdot}6H_2O$ (Merck), $Ag(NO_3)$ (Merck), $Mn(NO_3)_3{\cdot}4H_2O$ (Merck), $Cu(NO_3)_2{\cdot}3H_2O$ (Merck), citric acid, ethylene glycol according to the Pechini and sol–gel methods.

2-2. Pechini method

Nitrate salts were mixed in appropriate proportions and dissolved in deionized water. Citric acid was added to the nitrate solution at a citrate/metal molar ratio of 2:1. Then ethylene glycol (mass ratio of 40:60 to citric acid) [34] was added. The solution was heated at 70 °C with stirring. After water evaporation and polyesterification reaction between citric acid and ethylene glycol, the resin-like substance that formed was dried at 110 °C overnight and calcined at 750 °C for 4 h. The powders obtained were denoted P0 (x=0), P1 (x=0.1), P2 (x=0.2), and P3 (x=0.3).

2-3. Sol–gel method

The nitrates of La, Na and Cu were used as starting materials for obtaining an aqueous solution of La^{3+}, Ag^{+} ,$Mn^{4+/3+}$and Cu^{2+} with appropriate stoichiometry. The same amount of citric acid as for the Pechini method was added and the resulting solution was heated by constant stirring at temperatures of 70 °C. After water evaporation, the clear solution gradually turned to a milky sol and finally transformed into a gel. The gel was dried at 110 °C overnight and calcined at 750 °C for 4 h. The powders obtained were denoted S0 (x=0), S1 (x=0.1), S2 (x=0.2), and S3 (x=0.3).

It should be noted that S0 and P0 refer to $LaMn_{0.8}Cu_{0.2}O_{3\pm\delta}$ and the results are from our previous work [38].

2-4. Characterization and activity tests

Powder XRD patterns of the calcined perovskites before and after reactions were measured using a Philips PW-1800 diffractometer with Cu K_α radiation (λ=1.5406 Å) at 40 kV and 30 mA to

determine the crystalline phases and lattice parameters. Scanning was carried out over the 2θ range 5–90° with a step size of 0.03° and a count time of 2 s per step. Phase identification was carried out by comparison with Joint Committee on Powder Diffraction Standards (JCPDS) database cards.

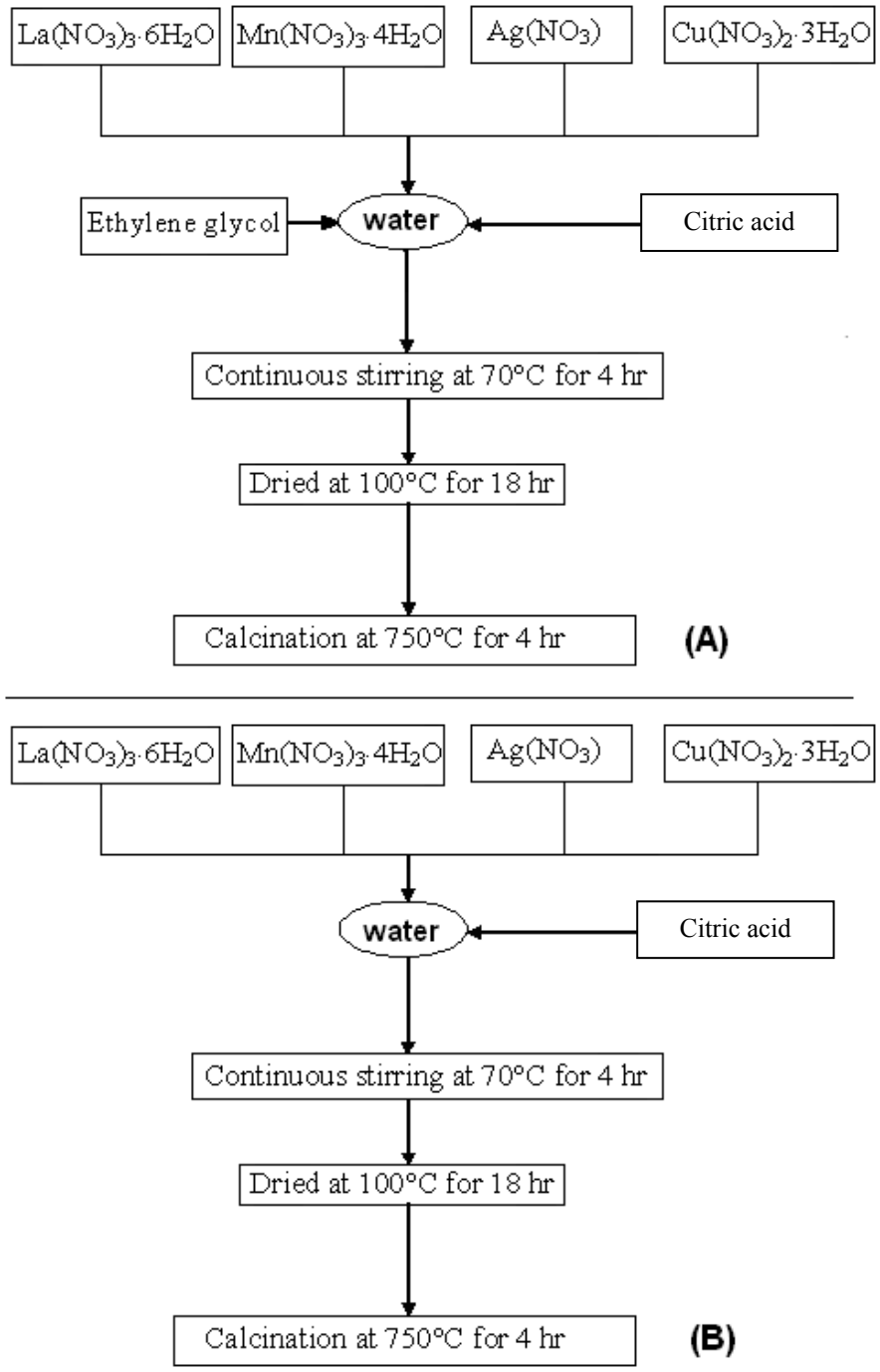

Figure 1. Schematic illustration of the preparation of $La_{1-x}Ag_xMn_{0.8}Cu_{0.2}O_{3\pm\delta}$ powders by (A) Pechini method, (B) sol-gel method

FT-IR spectra were recorded on a Shimadzu 8400s FT-IR instrument. The dried samples were dissolved in *n*-hexane then cooled to –10 °C. The crystals obtained were mixed at 3 wt.% with KBr and analyzed by FT-IR.

Catalyst compositions (by weight) were determined by XRF spectroscopy using a Thermo Scientific ARL ADVANT'X series instrument. The specific surface area of samples was measured by the BET isotherm technique for nitrogen adsorption on a BELCAT-A system operated in single-point mode. Temperature-programmed reduction (TPR) studies were performed on a BELCAT-A system equipped with a thermal conductivity detector (TCD) using calcined catalyst samples of approximately 100 mg. The samples were initially flushed with argon at a flow rate of 50 cm^3/min as the temperature was increased at 10 °C/min to 200 °C and then held for 60 min to remove water. The reducing gas (10% H_2 in argon) was introduced at a flow rate of 50 cm^3/min and the temperature was increased from room temperature to 1100 °C at 10 °C/min and then held for 70 min. The amount of hydrogen consumed was determined by TCD.

The morphology of calcined catalysts was examined by SEM using a VEGA II XMU electron microscope (TSCAN) operated in back-scattered and secondary electron detector modes to determine the morphology of the surface structures. The elemental analysis of the crystalline phases was determined by EDS coupled to the SEM.

Catalytic activity tests for methane combustion and CO oxidation were performed in a fixed-bed microreactor (I.D. 6.6 mm). Tests were carried out by feeding a mixture of 2 vol.% CH_4 and 10 vol.% O_2 in N_2 for methane combustion and 2 vol.% CO and 20 vol.% O_2 in N_2 for CO oxidation at 50 cm^3/min while the temperature was increased from 200 to 700 °C. A 0.2-g sample of catalyst was used for each test. Brooks (5850E) mass-flow controllers equipped with in-line filters and check valves were used to regulate the gas flows. The fixed-bed stainless steel reactor was placed in a cylindrical ceramic oven and was fed up flow. Analysis of the products and the feed components was performed by on-line gas chromatography using a Thermo Finnegan KAV00109 chromatograph with a TCD detector, helium as carrier gas, and a 5A 60/80 mesh molecular sieve.

3. Results and discussion

3-1. FT-IR spectroscopy

FT-IR spectra of $La_{1-x}Ag_xMn_{0.8}Cu_{0.2}O_{3\pm\delta}$ dried gels (x=0.1, 0.2, 0.3) prepared by both routes are presented in Fig. 2. As mentioned in Section 2.1, citric acid was used as the complexing agent for both routes. The bands detected at 1730cm^{-1}(▲) and 1080cm^{-1} (▲) are related to monodentate ligands containing a carbonyl group [35]. These bonds confirm complex formation between the complexing agent and metal ions. Peaks detected at approximately 1640cm^{-1}(■) and 1380cm^{-1} (■) for all samples are attributed to asymmetric and symmetric stretching modes of carbonyl groups, respectively [35, 36]. A wide band at approximately 3200 cm^{-1} (○) was detected for all samples, and is assigned to hydroxyl groups [35]. For the Pechini method, as ethylene glycol is used for polyesterification with citric acid to form a rigid polymer

network, a band related to C–O stretching was detected at approximately 1180 cm^{-1}(□), confirming the polymerization process [36, 37]. The FT-IR results thus confirm that complex formation between citric acid and metallic ions occurred in the sol–gel route and that polyesterification of ethylene glycol and citric acid and complexation with metallic ions occurred in the Pechini method.

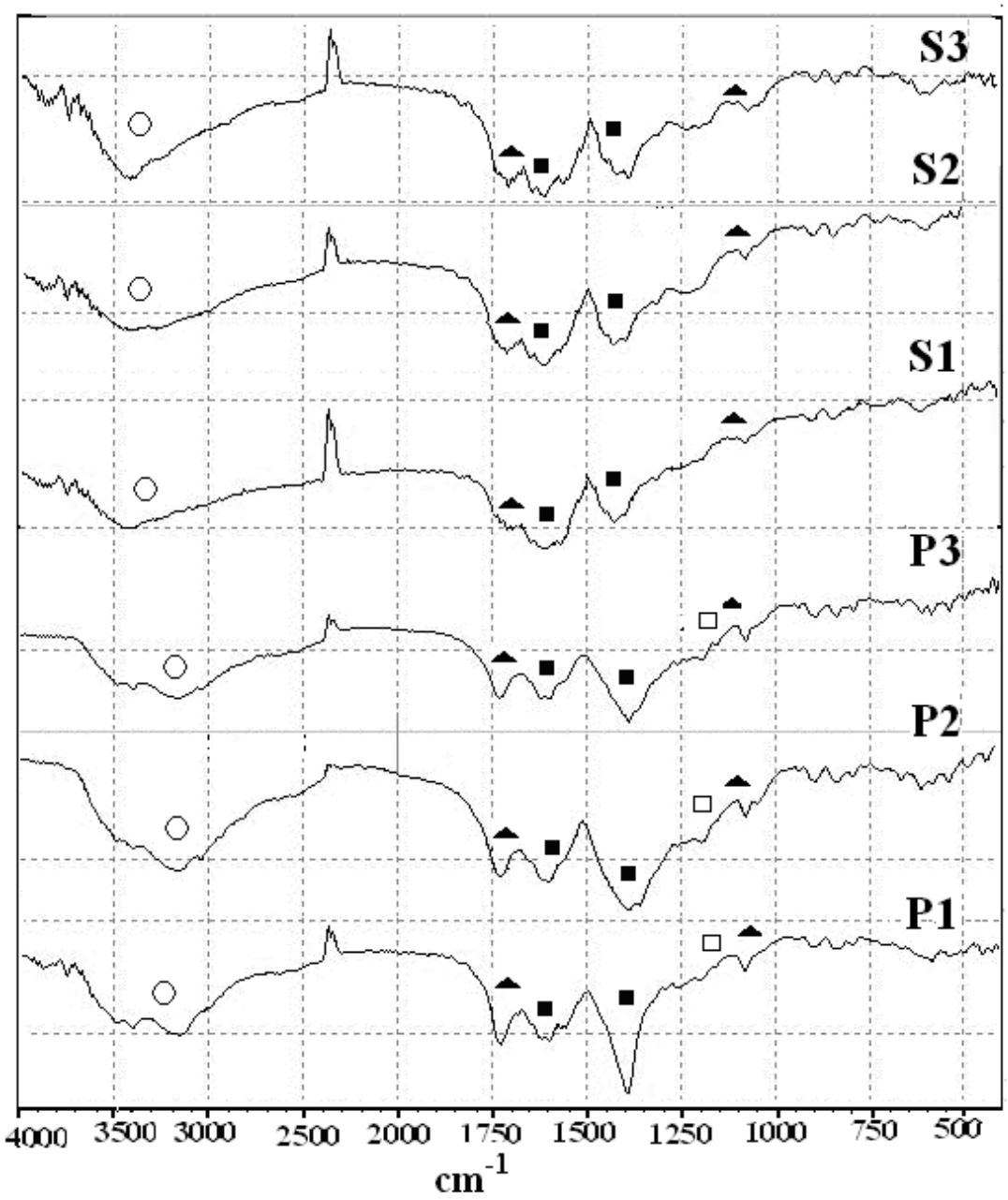

Figure 2. FTIR spectra of $La_{1-x}Ag_xMn_{0.8}Cu_{0.2}O_{3\pm\delta}$ precursor final solution prepared by Pechini (P1, P2, P3) and sol gel methods (S1, S2, S3)

3-2. XRD results

XRD measurements were performed to determine the crystalline structure of the calcined samples. XRD patterns of the perovskite oxides before and after catalytic tests are shown in Fig. 2A–B. For Pechini samples, only a single perovskite phase (JCPDS -33-0713) was detected for x=0, 0.1 and 0.2, but for x=0.3 metallic silver was detected in addition to the perovskite phase (Fig. 2A). The XRD patterns of the samples prepared by the sol–gel method are presented in Fig. 2B. Only a perovskite structure was detected for x=0 and 0.1, but both metallic Ag and a perovskite phase were detected for x=0.2 and 0.3. Comparison of the tolerance factor, t, for different samples prepared by the two methods reveals that, because of the smaller ionic radius of silver than lanthanum, t values deviated from 1, with increasing Ag substitution (x>0.2). This effect means that the perovskite structure becomes unstable for x>0.2, whereas for samples with x≤0.2 t is closer to 1 and the crystal structure is closer to cubic. Comparison of the XRD results indicates that the Pechini route leads to purer perovskite phases and that the sol–gel method leads to the formation of higher amounts of metallic Ag.

The lattice parameter calculated for all samples is shown in Table 1. For Pechini samples the lattice parameter decreased with increasing Ag, but no correlation was observed for sol–gel samples because this method yields greater separation of Ag from the perovskite structure and there is no estimate for silver introduction into a defined structure. Lower Ag segregation in Pechini samples is due to the usage of ethylene glycol, which leads to the formation of a rigid polymer network that suppresses the mobility of metal–citric acid complexes, which minimizes the segregation of metal particles during calcination.

The BET surface area was higher for Pechini samples than for sol–gel samples (Table 1). In both methods, the surface area of the samples increased with the Ag content, indicating that Ag can be helpful in increasing the surface area.

Table 1. Lattice parameter and surface area of perovskite- type oxides (In the table, P stands for samples prepared by Pechini method and S for samples prepared by sol-gel method and the general structure of samples is $La_{1-x}Ag_xMn_{0.8}Cu_{0.2}O_3$).

Samples	Lattice parameter (Å)	Surface area (m^2/g)
P0 ($LaMn_{0.8}Cu_{0.2}O_3$)	3.9708	14.0
P1 ($La_{0.9}Ag_{0.1}Mn_{0.8}Cu_{0.2}O_3$)	3.9707	16.0
P2 ($La_{0.8}Ag_{0.2}Mn_{0.8}Cu_{0.2}O_3$)	3.9690	17.0
P3 ($La_{0.7}Ag_{0.3}Mn_{0.8}Cu_{0.2}O_3$)	3.9650	17.5
S0 ($LaMn_{0.8}Cu_{0.2}O_3$)	3.9701	8.0
S1 ($La_{0.9}Ag_{0.1}Mn_{0.8}Cu_{0.2}O_3$)	3.9680	9.5
S2 ($La_{0.8}Ag_{0.2}Mn_{0.8}Cu_{0.2}O_3$)	3.9631	10.0
S3 ($La_{0.7}Ag_{0.3}Mn_{0.8}Cu_{0.2}O_3$)	3.9670	11.0

3-3. XRF, EDS and SEM results

The sample morphology was investigated by SEM before and after catalytic tests. Micrographs of samples S2 and P2 are shown in Fig. 3. The images reveal that the particle size of the sample prepared by the Pechini method was <200 nm, whereas particles of different sizes (up to 800 nm) were observed for the sol–gel sample. This confirms that the Pechini route leads to smaller particles than the sol–gel method. Fig. 3(c, d) shows micrographs of the same samples used in methane combustion reactions. The particle size of S2 was greater after the catalytic test due to sintering at higher temperatures during the reaction. After exposure to high temperature the particle size of P2 was in the range 50–300 nm, whereas particles in the order of micrometer were observed for S2. SEM images of other samples (data not shown) also reveal that the particle size of Pechini samples was less sensitive to high temperatures, and these samples showed more resistance to high temperatures. SEM investigations after activity tests thus demonstrate that Pechini samples were less agglomerated and retained a fine crystal size, whereas the corresponding sol–gel samples exhibited a greater particle size.

Sample homogeneity was investigated by EDS at different sample points before and after catalytic tests. The weight percent of different elements was determined by XRF. As an example, XRF and EDS results for samples S2 and P2 are presented in Table 2.

For P2 the weight percent of different elements was similar at different points, indicating a uniform distribution of elements. The results are also close to the theoretical values. However, different values of Ag wt.% were obtained at three points for S2, which differ from the theoretical value. The reason is that at x=0.2 for sol–gel samples, only some of the Ag entered the perovskite structure and the remainder forms a metallic phase, as revealed by XRD. The XRF results also correspond to theoretical values.

Comparison of EDS results after catalytic tests also indicates that the distribution of different elements was more uniform and closer to the theoretical values for P2 than for S2.

Table 2. EDS average values and XRF data of P2 and S2 samples before and after activity test

Element	P2				S2			
	La	Ag	Mn	Cu	La	Ag	Mn	Cu
Theoretical	58.66	11.38	23.29	6.72	58.66	11.38	23.29	6.72
XRF	59.60	10.85	23.20	6.35	59.95	10.05	23.45	6.55
EDS (Fresh catalyst)	59.21	10.01	23.64	7.13	58.35	7.98	23.61	8.53
EDS (after Activity test)	61.10	8.92	23.11	6.89	62.02	6.49	23.18	6.67

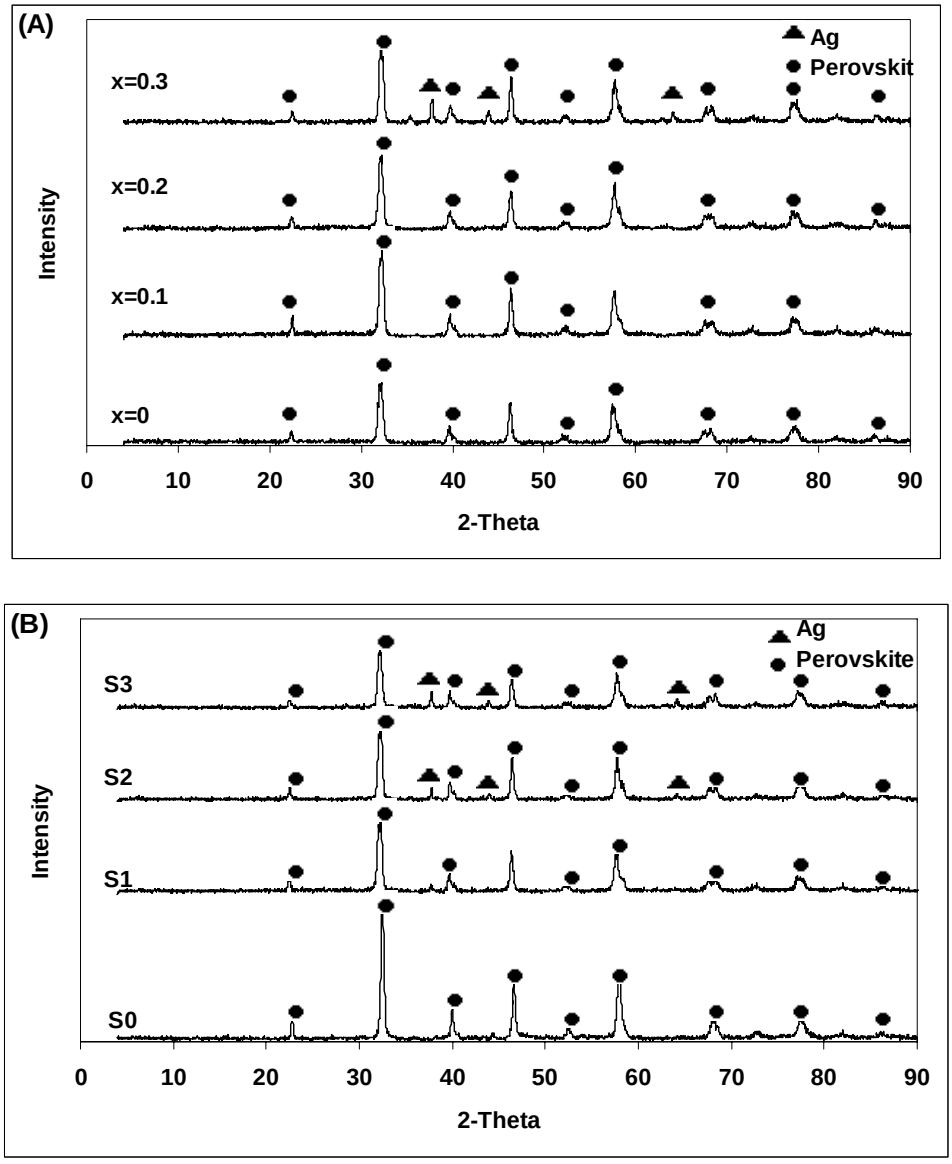

Figure 3. XRD patterns of $La_{1-x}Ag_xMn_{0.8}Cu_{0.2}O_{3\pm\delta}$ perovskite calcined at 750°C for 4 hours; prepared by (A) Pechini method before and (B) sol gel method

3-4. TPR

Fig. 4 shows TPR profiles of $La_{1-x}Ag_xMn_{0.8}Cu_{0.2}O_{3\pm\delta}$ (x=0, 0.1, 0.2, 0.3) catalysts prepared by the Pechini and sol–gel methods. Two main peaks were detected in all cases; one at temperatures ranging from 200 to 300 °C and the other at temperatures between 800–900°C. XRD results of the samples after TPR, confirm the presence of metallic Cu, metallic Ag, MnO and La_2O_3. Therefore the first peak is dedicated to Cu^{2+}, and Mn^{4+} reduction to Cu° and Mn^{3+}, respectively, and the second peak to the reduction of Mn^{3+} to Mn^{2+} as also observed by L.Lisi [32]. For samples S0 and P0 without Ag, the first reduction peak was at approximately 240 °C. Substitution of 10% Ag in the A site increased the stability of the perovskite structure and therefore the reduction peak shifted to a higher

temperature (280 °C for P1 and 300 °C for S1). Higher Ag substitution at x=0.2 decreased the stability of the structure, so P2 and S2 samples were reduced at lower temperatures than for P1 and S1. At x=0.3 the reduction temperature of the Pechini sample further decreased. However, for sample S3 there was little difference in reduction temperature compared to S2. According to the XRD results for S3, only some of the Ag enters the perovskite structure, similar to S2, and the rest is metallic Ag on the surface.

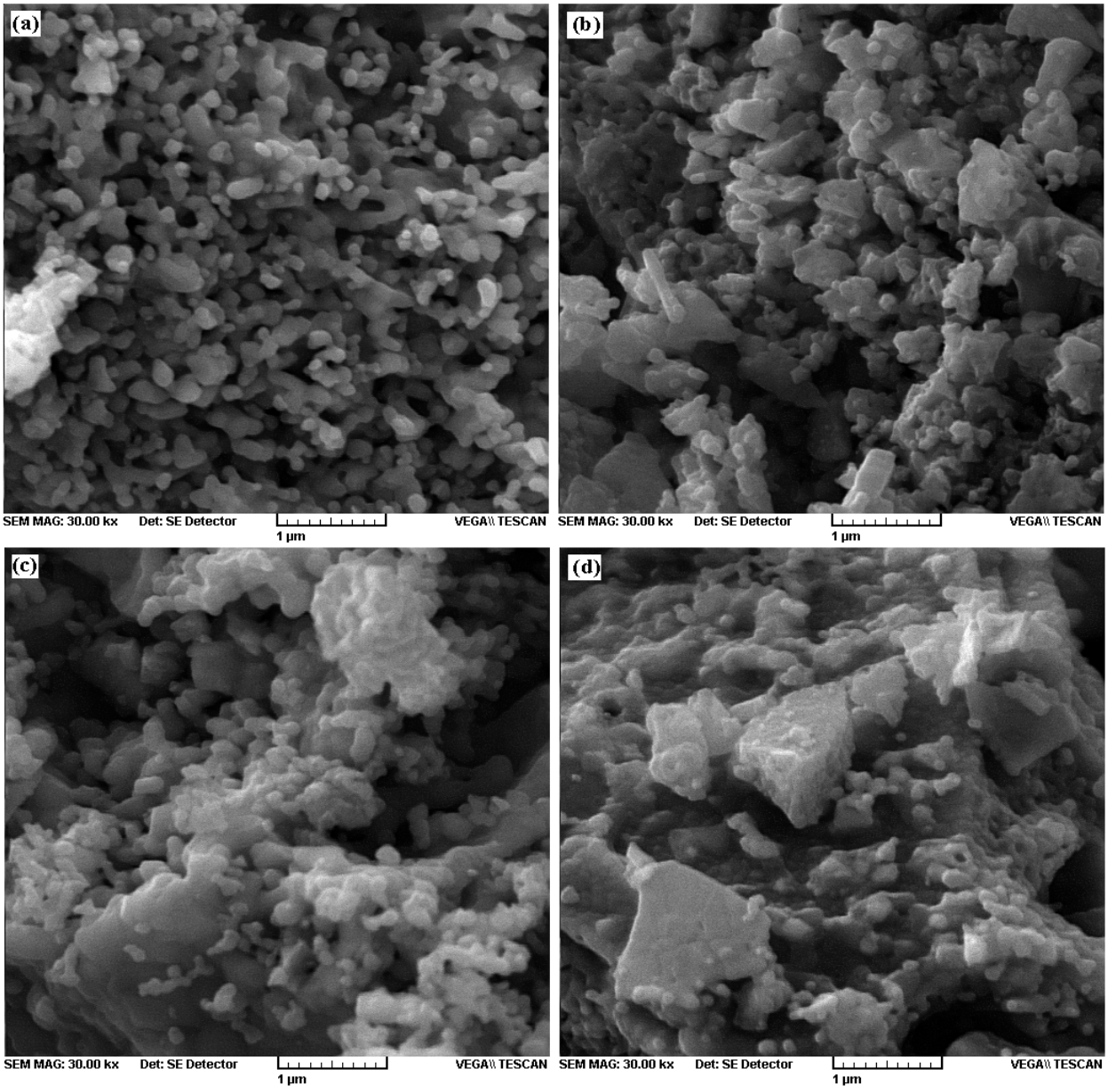

Figure 4. SEM images of (a) fresh P2 sample; (b) fresh S2 sample ;(c) P2 sample after activity test; (d) S2 sample after activity test

Comparison of the TPR results revealed that the Pechini samples were reduced at a lower temperature and had higher hydrogen consumption than the sol–gel samples. Hydrogen consumption for the samples was 3.25, 3.54, 3.88 and 3.92 mmol/g for P0–P3 and 2.83, 3.1, 3.64 and 3.78 mmol/g for S0–S3, respectively. Since most of the Ag enters the perovskite structure in Pechini samples, hydrogen consumption is higher and reduction can occur at a lower temperature. According to the hydrogen consumption for these samples, the correct formula and Mn^{4+}/Mn^{3+} ratio can be calculated. Thus, the formula for mixed oxides prepared by the Pechini method is $La_{1-x}Ag_yMn^{3+}{}_{0.4}Mn^{+4}{}_{0.4}Cu_{0.2}O_{3\pm\delta}$. These results indicate that as the amount of silver increased from x=0 to x=0.3, δ decreased from 3.1 to 2.8, respectively.

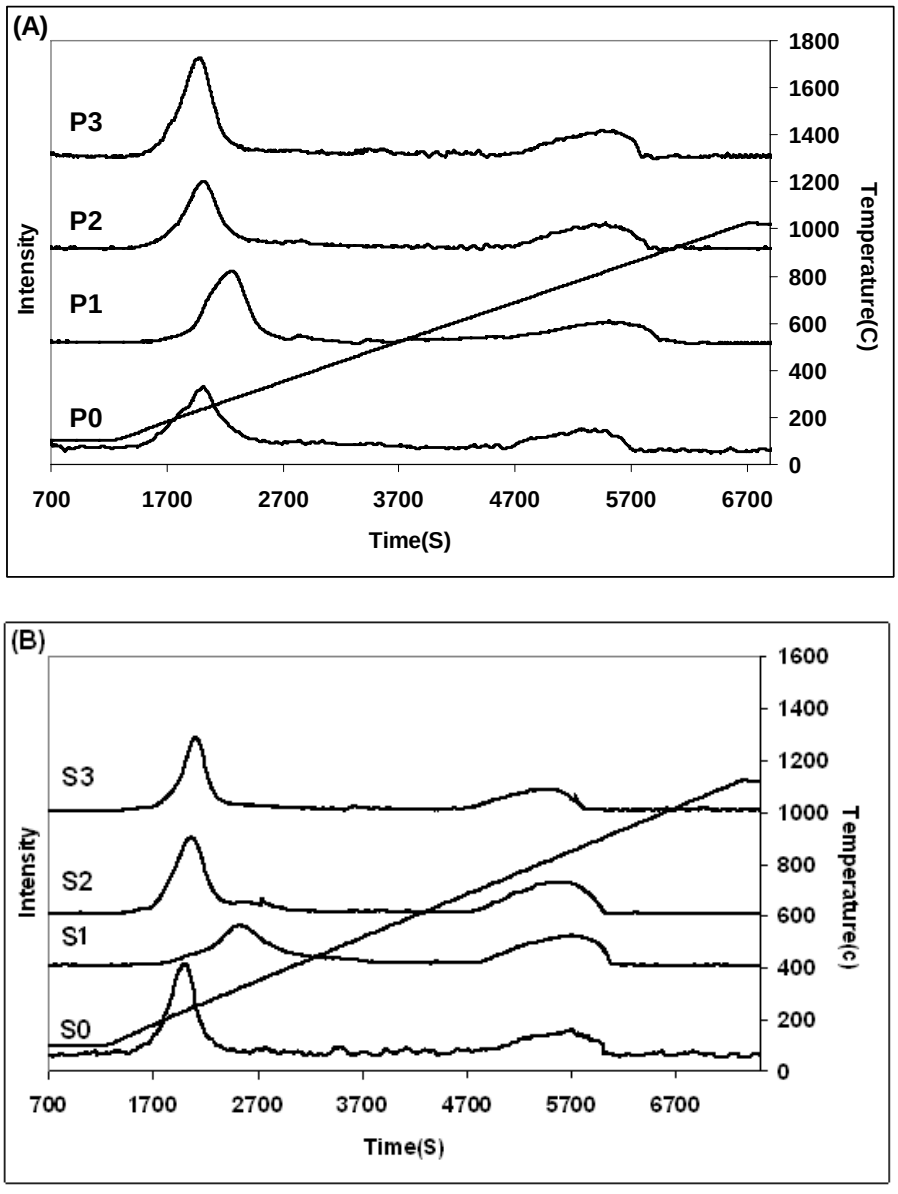

Figure 5. TPR Profile of Pechini (P0, P1, P2, P3) and Sol-gel (S0, S1, S2, S3) samples

3-5. Activity tests

Catalytic activity test results of the samples in methane combustion and CO oxidation are shown in Fig. 6 (A, B) and Fig.7 (A, B), respectively. As can be seen, the samples without Ag prepared by both methods had lower activities in comparison with the samples containing Ag. By increasing the Ag content of the samples the catalytic activity is improved, because by increasing the Ag content, trivalent La is substituted by silver (1+) and this difference in the valences of the elements leads to the deficiency of the perovskite structure which is the reason for better reduction and higher activities of the samples containing higher amounts of Ag. At x=0.2 and 0.3 the catalytic activity of the samples were similar. The samples prepared by the Pechini method were more active than the samples prepared by the sol-gel method. $T_{50\%}$ and $T_{90\%}$ of the samples in methane combustion and CO oxidation reaction, are shown in Fig 8(A, B). The reason for the higher activity of the Pechini samples is their smaller particle sizes and higher surface areas. Also, according to XRD results in the Pechini method most of the silver enters the perovskite structure which leads to higher deficiency of the perovskite structure and higher activity.

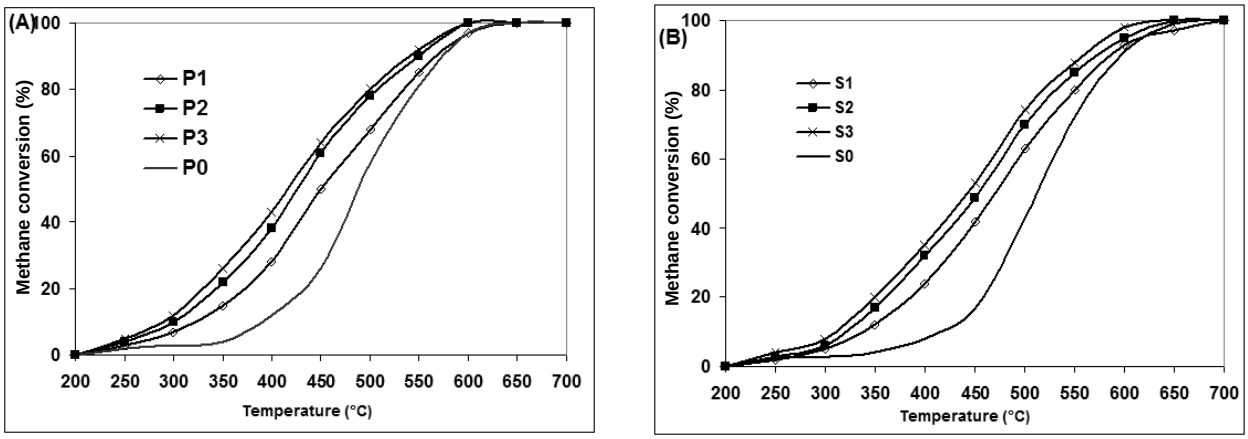

Figure 6. Methane conversion of Pechini (P0, P1, P2, P3) and Sol-gel (S0, S1, S2, S3) samples

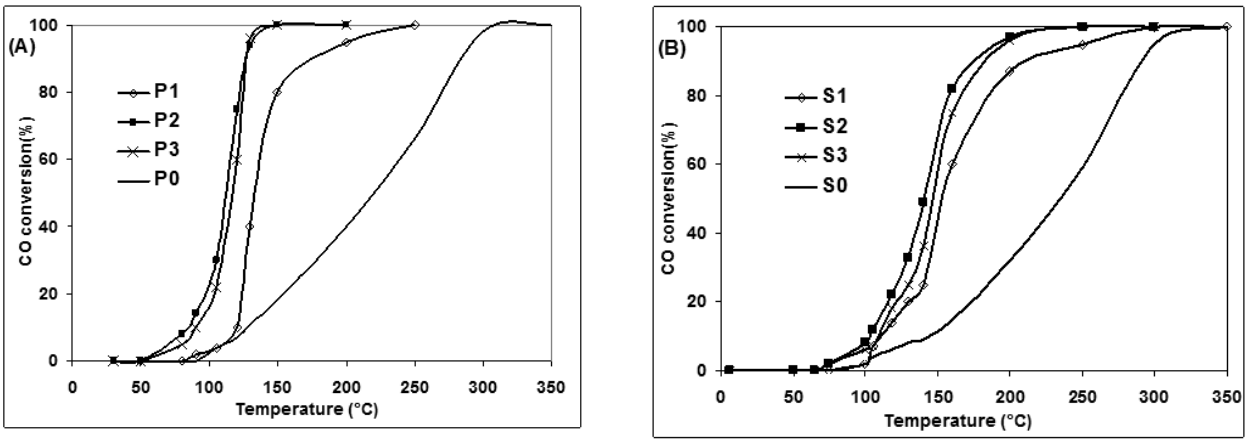

Figure 7. Activities of Pechini (P0, P1, P2, P3) and Sol-gel (S0, S1, S2, S3) samples for CO oxidation at different reaction temperatures

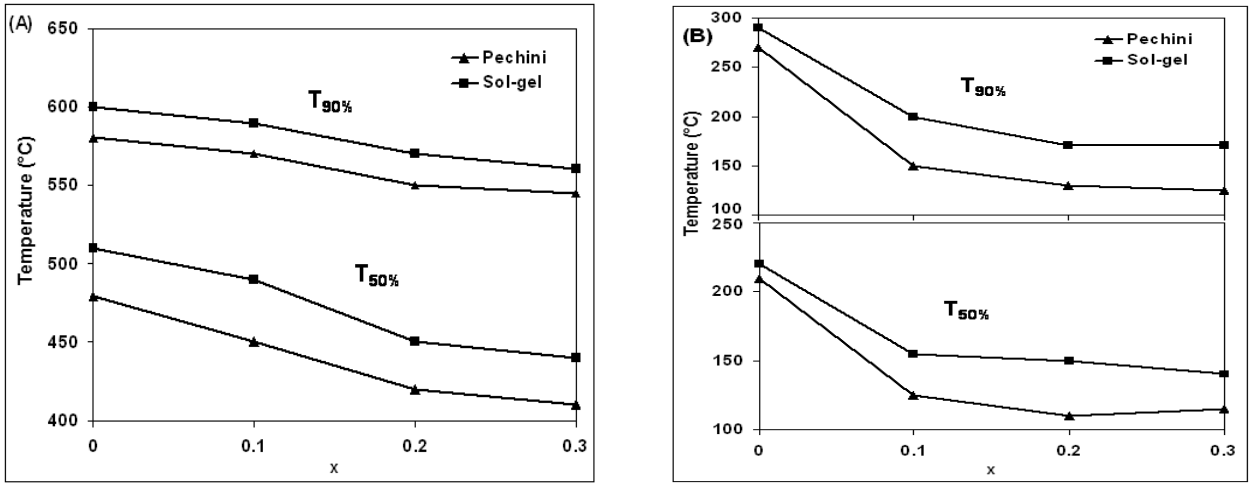

Figure 8. $T_{50\%}$ and $T_{90\%}$ of Pechini (P0, P1, P2, P3) and Sol-gel (S0, S1, S2, S3) samples in (A): methane combustion and (B) : CO oxidation reaction

The CO oxidation results indicate that Ag addition to $LaMn_{0.8}Cu_{0.2}O_{3\pm\delta}$ greatly improved the catalytic activity. The CO total conversion temperature of sample P2 was approximately 200 °C lower than that of P0. Comparison of results of the Ag-containing samples revealed that P2 and S2 had the highest activity among the Pechini and sol–gel samples, respectively, in agreement with the TPR results. Similar to observations for methane conversion, Pechini samples were more active than the sol–gel samples for CO oxidation.

3-6. XRD results after activity testing

The XRD results of the samples after methane combustion activity tests is shown in Fig. 9A,B. These results were compared with the XRD patterns of the samples before catalytic tests, in order to investigate changes in structure. After activity tests, Pechini samples with Ag substitution of <20% had approximately the same XRD spectra as before, and for x=0 (no silver substitution) the spectra before and after the tests were exactly the same for samples prepared by both methods. Peaks for the sol–gel samples indicate the presence of silver in metallic form besides the perovskite phase. For sol–gel samples, peaks related to non-perovskite phases increased with the Ag content, indicating that silver migrated from the perovskite structure after exposure to reaction conditions and a metallic phase was formed. Comparison of XRD results for the Pechini and sol–gel samples revealed lower Ag segregation during catalytic tests for the former; the initial structure was maintained and therefore the Pechini samples were more stable. Due to the lower temperatures necessary for complete CO oxidation on $La_{1-x}Ag_xMn_{0.8}Cu_{0.2}O_{3\pm\delta}$ oxides and their structural stability at those temperatures, no changes were observed in the structure of the oxides after CO oxidation tests.

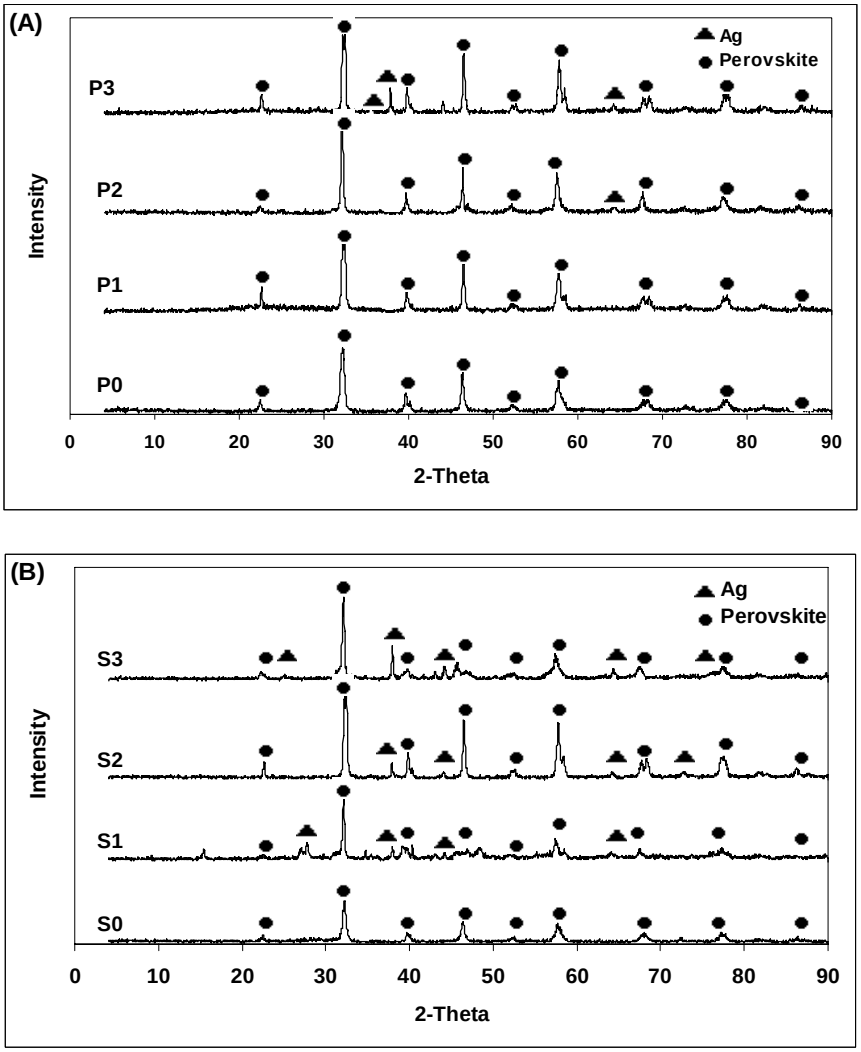

Figure 9. XRD patterns of $La_{1-x}Ag_xMn_{0.8}Cu_{0.2}O_{3\pm\delta}$ perovskite prepared by (A) Pechini method and (B) sol gel method after methane combustion activity test

4. Conclusions

$La_{1-x}Ag_xMn_{0.8}Cu_{0.2}O_{3\pm\delta}$ (x=0, 0.1, 0.2, 0.3) perovskites were prepared by two different methods, the Pechini and sol–gel methods. XRD results for calcined samples showed that more silver entered the structure in the Pechini samples than in the sol–gel samples. Samples prepared by the Pechini method had higher surface area and lower particle size than those prepared by the sol–gel method. The Pechini samples exhibited a uniform distribution of elements at different points that was close to the theoretical values. The catalytic activity of the oxides was investigated for methane combustion and CO oxidation reactions. The Pechini samples had higher activity for both reactions. The catalytic activity increased with the Ag content for samples prepared by both methods. At x=0.2 and 0.3 the catalytic activity of the samples was similar. For CO oxidation the catalytic activity of the Pechini samples was higher and Ag substitution increased the activity of the oxides.

Comparison of XRD results for the oxides before and after catalytic tests revealed that Ag reduced at higher temperatures could not return to the bulk after catalysis test in sol–gel samples, and therefore Ag remained in the metallic phase on the perovskite. However, in Pechini samples only a small proportion of the silver remained on the surface and most of it returned to the bulk, thus conferring higher stability to these samples. In terms of activity and XRD results, $La_{0.8}Ag_{0.2}Mn_{0.8}Cu_{0.2}O_{3\pm\delta}$ prepared by both methods was the most active and stable sample.

References

[1] Choudhary, T. V., Banerjee, S. and Choudhary, V. R., "Catalysts for combustion of methane and lower alkanes", Appl. Catal. A., 234, 1, (2002).

[2] Piotrowska, A.M. and Landmesser, H., "Noble metal-doped perovskites for the oxidation of organic air pollutants", Catalysis Today, 137, 355, (2008).

[3] Levasseur, B. and Kaliaguine, S., "Effect of the rare earth in the perovskite-type mixed oxides" , Journal of Solid State Chemistry, 181, 2953, (2008).

[4] Cimino, S., Lisi, L., Rossi, S.D., Faticanti, M. and Porta, P., "Methane combustion and CO oxidation on $LaAl_{1-x}Mn_xO_3$ perovskite-type oxide solid solutions", Applied Catalysis B: Environmental.,43 , 397, (2003).

[5] Ifrah, S., Kaddouri, A., Gelin, P. and Leonard, D., "Conventional hydro-thermal process versus microwave-assisted hydrothermal synthesis of $La_{1\_x}Ag_xMnO_3$ perovskites used in methane combustion"., C. R. Chimie., 10 , 1216, (2007).

[6] Feng, L.M., Jiang, L.Q., Zhu., Liu, H.B., Zhou, X. and Li, C.H., "Formability of ABO_3 cubic perovskites", J. Phys. Chem . Solids, 69, 967, (2008).

[7] Porta, P., Rossi, S.D., Faticanti, M. and Minelli, G., "Perovskite-Type Oxides". Journal of Solid State Chemistry.,146, 291, (1999).

[8] Ullmann, H. and Trofimenko, N., "Estimation of effective ionic radii in highly defective perovskite-type oxides from experimental data", J .Alloys. Compounds, 316, 153, (2001).

[9] Kattack,, C. P. and Wang, F.F.Y., Handbook of the physics and chemistry of rare Earths, K. A. Gschneider, L. Enging Eds., North Holland Publ., Amsterdam, p.525, (1979).

[10] Li, C., Kwan Soh, K. Ch. and Wu, P., "Formability of ABO_3 perovskites", J. Alloys . Compounds,40, 372, (2004).

[11] Spinicci, R., Delmastro, A., Ronchetti, S. and Tofanari, A., "Catalytic behaviour of stoichiometric and non-stoichiometric $LaMnO_3$ perovskite towards methane combustion", Materials Chemistry and Physics.,78, 393, (2003).

[12] Kharton, V. V., Viskupa, A. A., Naumovicha, E. N. and Tikhonovicha, V.N., "Oxygen permeability of $LaFe_{1-x}Ni_xO_{3-\delta}$ solid solutions". Materials Research Bulletin., 34, 1311, (1999).

[13] Cui, H., Zayat, M. and Levy, D., "Epoxide assisted sol–gel synthesis of perovskite-type $LaM_xFe_{1\_x}O_3$ nanoparticles". J. Non-Crystalline Solids., 352, 3035, (2006).

[14] Choudhary, V.R., Uphade, B.S. and Pataskar, S.G., "Low temperature complete combustion of methane over Ag-doped $LaFeO_3$ and $LaFe_{0.5}Co_{0.5}O_3$ perovskite oxide catalysts". Fuel.,78,919, (1999).

[15] Pi, L., Hervieu, M., Maignan, A., Martin, C. and Raveau, B., "Structural and magnetic phase diagram and room temperature CMR effect of $La_{1-x}Ag_xMnO_3$". Solid State Communications. 126, 229, (2003).

[16] Song, K., Cui, H., Kim, S. and Kang, S., "Catalytic combustion of CH_4 and CO on $La_{1-x}M_xMnO_3$ perovskites". Catalysis Today.,47, 155, (1999).

[17] Forni, L. and Rossetti, I., "Catalytic combustion of hydrocarbons over perovskites". Applied Catalysis B: Environmental., 38, 29, (2002).

[18] Singh, RN., Shivakumara, C., Vasanthacharya, N.Y., Subramanian, S. and Hegde, M.S., "Synthesis, structure, and properties of Sodium or Potassium-doped Lanthanum orthomanganites from NaCl or KCl flux". J. solid state chemistry.,137, 19, (1998).

[19] Ghigna, P., Carollo, A., Malavasi, L. and Subias, G., "Local structure and electronic properties of the rhombohedral and orthorhombic colossally magnetoresistive manga-nites $La_{1-x}Na_xMnO_3$ by Mn−K edge EXAFS and XANES". Journal Phys. Chem. B, 109, 4365, (2005).

[20] Malavasi, L., Mozzati, M.C., Tullio, E., Tealdi, C. and Flor, G., "Redox behavior of Ru-doped $La_{1-x}Na_xMnO_{3+d}$ manga-nites". physical review.,71, 174435, (2005).

[21] Fabbrini, L., Kryukov ,A., Cappelli, S., Chiarello, G.L., Rossetti, I., Oliva, C. and Forni, L., "$Sr_{1-x}Ag_xTiO_{3\pm\delta}$ (x=0, 0.1) perovskite-structured catalysts for the flameless combustion of methane". Journal of Catalysis., 232, 247, (2005).

[22] Steenwinkel, Y. Zh., Beckers, J. and Bliek, A., "Surface properties and catalytic performance in CO oxidation of cerium substituted lanthanum–manganese oxides". Applied Catalysis A: General., 23, 79, (2002).

[23] Kucharczyk, B. and Tylus, W., "Effect of Pd or Ag additive on the activity and stability of monolithic $LaCoO_3$ perovskites for catalytic combustion of methane". Catalysis Today., 90, 121, (2004).

[24] Gularia, E., Gueldue, C., Srivannavit, S. and Osuwan, S., "Co oxidation by silver cobalt composite oxide". Applied Catalysis A: General., 182, 147, (1999).

[25] Kirchnerova, J. and Klvana, D., "Synthesis and characterization of perovskite catalysts". Solid State Ionics., 12, 307, (1999).

[26] Liu, Zh., Hao, J., Fu, L. and Zhu, T., "Study of $Ag/La_{0.6}Ce_{0.4}CoO_3$ catalysts for direct decomposition and reduction of nitrogen oxides with propene in the presence of oxygen", Applied Catalysis B: Environmental., 44, 355, (2003).

[27] Tian, Zh.Q., Yu, H.T. and Wang, Zh.L., "Combustion synthesis and characterization of nano crystalline $LaAlO_3$ powders". Materials Chemistry and Physics., 106, 126, (2007).

[28] Civera, A., Pavese, M., Saracco, G. and Specchia, V., "Combustion synthesis of perovskite-type catalysts for natural gas combustion". Catalysis Today., 83, 199, (2003).

[29] Kakihana, M., Arima, M., Yoshimura, M., Ikeda, N. and Sugitani, Y., " Synthesis of high surface area LaMnO by a polymerizable complex method". J. Alloys and Compounds., 283, 102, (1999).

[30] Tabata, K., Hirano, Y. and Suzuki, E., "XPS studies on the oxygen species of $LaMn_{1-x}Cu_xO_3$". Applied Catalysis A: General., 170, 245, (1998).

[31] Zhang, R., Villanueva, A., Alamdari, H. and Kaliaguine, S., "Reduction of NO by CO over nanoscale $LaCo_{1-x}Cu_xO_3$ and $LaMn_{1-x}Cu_xO_3$ perovskites". J. Molecular Catalysis A: Chemical., 258, 22, (2006).

[32] Lisi, L., Bagnasco, G., Ciambelli, P., Rossi, S. and Porta, P., "Perovskite-type oxides". J. Solid State Chemistry., 146, 176, (1999).

[33] Zhang, R., Villanueva, A., Alamdari, H. and Kaliaguine., S., "SCR of NO by propene over nanoscale $LaMn_{1\_x}Cu_xO_3$ perovskites". Applied Catalysis A: General., 307, 85, (2006).

[34] Melo, D. M. A., Borges, F. M. M., Ambrosio, R.C. and Pimentel, P. M., "XAFS characterization of $La_{1\_x}Sr_xMnO_{3\pm d}$ catalysts prepared by Pechini method". Chemical Physics., 322, 477, (2006).

[35] Yang, W.D., Chang, Y.H. and Huang, Sh. H., "Influence of molar ratio of citric acid to metal ions on preparation of $La_{0.6}7Sr_{0.33}MnO_3$ materials via polymerizable complex process". J. European Ceramic Society., 25, 3611, (2005).

[36] Worayingyong, A., Kangvansura, P., Ausadasuk, S. and Praserthdam, P., "The effect of preparation: Pechini and Schiff base methods, on adsorbed oxygen of $LaCoO_3$ perovskite oxidation catalysts". Colloids and Surfaces A: Physicochem. Eng. Aspects., 315, 217, (2008).

[37] Wang, S., Zhang, Y. A., Zhang, Z. and Qian, Y., "Ethanothermal reduction to MoO2 microspheres via modified Pechini method", J. crystal Growth., 293, 209, (2006).

[38] Abdolrahmani, M., Parvari, M. and Habibpoor, M., "Effect of Copper substitution and preparation methods on the $LaMnO_{3\pm d}$ structure and catalysis of Methane combustion and CO oxidation"., Chines Journal of Catalysis. 31, 394, (2010).